Automatic Methodology for Wideband Power Amplifier Design

Catarina Belchior, *Graduate Student Member, IEEE*, Luís C. Nunes, *Member, IEEE*, Pedro M. Cabral, *Senior Member, IEEE*, and José C. Pedro, *Fellow, IEEE*

***Abstract*— This letter presents an automatic power amplifier (PA) design methodology that uses a multidimensional search algorithm to find the best compromise between fundamental and harmonic impedance terminations for a specified bandwidth. In conventional design methodologies, PA designers need to preselect the optimum impedances, which normally follow non-Foster trajectories, and are thus impossible to achieve with passive matching networks (MNs) for a wide frequency range. Instead, the proposed automatic design method directly synthesizes the MNs to achieve the desired output power, efficiency, and gain performance, without forcing any impedance profiles. For that, load-pull data are interpolated using artificial neural networks and an algorithm based on the simplified real frequency technique is used to obtain the MNs. Finally, the method is validated with a single-ended PA implementation.**

***Index Terms*— Automatic power amplifier (PA) design, optimum PA matching, PAs, simplified real frequency technique (SRFT), wideband.**

I. Introduction

In WIRELESS communication systems, RF power amplifiers (PAs) assume an essential role and should be designed to improve specific performance metrics such as efficiency, output power (P_{out}), gain, and bandwidth. Traditionally, highly trained PA designers preselect a profile of load impedance versus frequency that, based on their accumulated experience, is believed to meet the desired goals, and then use optimization tools to approximate that profile.

Over time, the simplified real frequency technique (SRFT) [1] has been widely used as a broadband design technique and is further developed so that it could include harmonic control [2], [3]. However, since the optimization cost functions of these techniques are formulated considering non-Foster target impedances, suboptimal solutions will be achieved, significantly affecting the PA's efficiency and P_{out}.

Alternatively, P_{out} and efficiency metrics could be directly optimized using a nonlinear model and computer-aided design simulators [4], [5]. Unfortunately, this solution introduces several convergence issues, making the process slow, and most of the time, failing to obtain the optimum solution, especially for wideband designs where high-order matching networks (MNs) are used. To tackle this issue, distinct techniques have been proposed [6]–[8]; however, they all neglect the PA performance change with harmonic terminations.

The proposed design method aims to solve the mentioned issues and to provide an automatic way to design the PA MNs given the source- and load-pull terminations for gain, P_{out}, and efficiency. On the one hand, the MNs are directly optimized to obtain these desired performance metrics, without the need for the designer to preselect the optimum impedances. On the other hand, there is no need to use the traditional slow and cumbersome nonlinear optimizations, since an automatic multidimensional search algorithm is used to find the best compromise between fundamental and harmonic impedances.

II. Proposed Automatic PA Design Methodology

Currently, source- and load-pull measurements are one of the most used active device characterization data, preferred by both vendors and PA designers, broadly available for any new device technology being the core of our PA design methodology procedure, which we will describe step-by-step in this section and is summarized in the flowchart (Fig. 1).

A. Step 1: Source- and Load-Pull Data Interpolation

In this first step, the objective is to build functions that map the discrete efficiency, P_{out}, and gain values, obtained from measurements (after a standard interpolation procedure), to the source and load impedances presented to the active device. Since fundamental and second-harmonic load terminations (Γ_{L1H} and Γ_{L2H}, respectively) have a direct impact on the active device efficiency and output power contours, and the fundamental source and load terminations (Γ_{S1H} and Γ_{L1H}, respectively) will impact the small-signal gain, we divided this mapping into two separate functions in the following equations:

$$\left[\text{Eff}_{3\,\text{dB}}, P_{\text{out}_{3\,\text{dB}}}\right] = F_{\text{ANN1}}(\Gamma_{L1H}, \Gamma_{L2H}) \quad (1)$$

$$\text{Gain}_{\text{SS}} = F_{\text{ANN2}}(\Gamma_{L1H}, \Gamma_{S1H}) \quad (2)$$

where $\text{Eff}_{3\,\text{dB}}$ and $P_{\text{out}_{3\,\text{dB}}}$ correspond to the efficiency and output power at 3 dB compression and Gain_{SS} to the small-signal gain. To build these functions, an artificial neural network (ANN), with two layers and 15 neurons each, was used.

B. Step 2: Final PA Goal Specification ($Gain_{SS}$, $Eff_{3\,dB}$, and $P_{out_{3\,dB}}$)

The desired goals for small-signal gain, efficiency, and output power at 3 dB compression should be defined, having in mind the final PA operation regime.

Manuscript received March 25, 2021; revised May 6, 2021; accepted May 19, 2021. Date of publication May 24, 2021; date of current version August 9, 2021. This work was supported by the Fundação para a Ciência e Tecnologia (FCT)/Ministério da Educação e Ciência (MEC) through the National Funds under Project PTDC/EEI-TEL/30534/2017. The work of Catarina Belchior was supported in part by FCT through Fundo Social Europeu (FSE) and in part by the Programa Operacional Regional do Centro under Grant SFRH/BD/05414/2020. *(Corresponding author: Catarina Belchior.)*

The authors are with the Departamento de Eletrónica, Telecomunicações e Informática (DETI), Instituto de Telecomunicações, Universidade de Aveiro, 3810-193 Aveiro, Portugal (e-mail: c.belchior@ua.pt; cotimos@ua.pt; pcabral@ua.pt; jcpedro@ua.pt).

Color versions of one or more figures in this letter are available at https://doi.org/10.1109/LMWC.2021.3083101.

Digital Object Identifier 10.1109/LMWC.2021.3083101

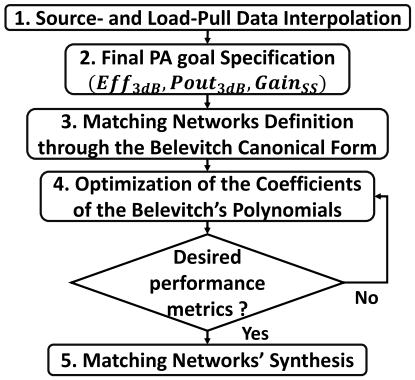

Fig. 1. Proposed PA design methodology.

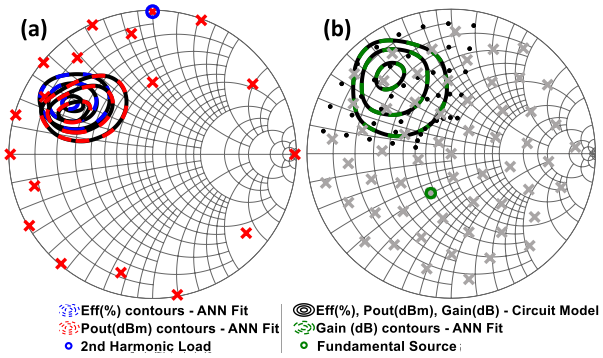

Fig. 2. Comparison between (a) efficiency, P_{out} (at 3 dB compression), and (b) small-signal gain contours from the circuit and ANN models at 2.4 GHz.

C. Step 3: MNs Definition Through the Belevitch Canonical Form

According to the well-known Belevitch canonical form used by SRFT, the S-parameters of a two-port network can be defined by a set of polynomials in Richard's domain [9]. In this regard, the so-called $f(\lambda)$ and $h(\lambda)$ polynomials, describing the PA's input and output MNs (IMN and OMN, respectively), should be defined. After this, the $g(\lambda)$ polynomial can be determined through the lossless condition [9].

D. Step 4: Belevitch's Polynomial Coefficients Optimization

From [9], the $S_{11}(\lambda)$ of IMN and OMN is defined as $h(\lambda)/g(\lambda)$, which, in turn, can be used as inputs of F_{ANN1} and F_{ANN2}. In this sense, it is possible to incorporate the polynomials that define the MNs in the extracted ANN models, thus constructing an error function in which output power, efficiency, and gain are the goals, as follows:

$$\begin{aligned} F = \sum_{i=1}^{N} & \left(\text{Eff}_{3\,\text{dB}} - F_{\text{ANN1}} \left(\frac{h_{\text{omn}}(\lambda)}{g_{\text{omn}}(\lambda)}, \frac{h_{\text{omn}}(\lambda_2)}{g_{\text{omn}}(\lambda_2)} \right) \right)^2 \\ & + \left(P\text{out}_{3\,\text{dB}} - F_{\text{ANN1}} \left(\frac{h_{\text{omn}}(\lambda)}{g_{\text{omn}}(\lambda)}, \frac{h_{\text{omn}}(\lambda_2)}{g_{\text{omn}}(\lambda_2)} \right) \right)^2 \\ & + \left(\text{Gain}_{\text{SS}} - F_{\text{ANN2}} \left(\frac{h_{\text{omn}}(\lambda)}{g_{\text{omn}}(\lambda)}, \frac{h_{\text{imn}}(\lambda)}{g_{\text{imn}}(\lambda)} \right) \right)^2 \end{aligned} \tag{3}$$

where λ_2 is Richard's variable for the second harmonic and N denotes the number of frequency points. In this step, $h(\lambda)$ coefficients should be optimized according to (3).

E. Step 5: Matching Networks' Synthesis

Due to the MNs canonical form, Richard's synthesis theory and removal criterion can be used (details can be found in [10]). At the end, the characteristic impedances and frequencies of each transmission line are determined.

The proposed algorithm automatizes both the optimum impedance profile search and PA design. It uses a multidimensional search algorithm to find the best combination between fundamental and harmonic impedance terminations, considering the MNs' realizability. This methodology presents clear advantages when compared with conventional methods where the impedance profiles need to be upfront selected without knowing if there is an MN that can reproduce them. The optimal solution is not guaranteed and depends on the designer's experience to select the best realizable impedance profiles.

Besides that, several important aspects of the proposed methodology can be highlighted.

1) The procedure is uniquely based on source- and load-pull data to build (1) and (2), which means that having a nonlinear circuit model for the active device is not necessary.
2) Contrary to what is determined in [4] and [5], our method avoids the slow and cumbersome nonlinear optimization over harmonic balance simulations.
3) The fact that the fundamental and second-harmonic load terminations are inputs of F_{ANN1} functions provides a multidimensional search method that guarantees the best compromise between them, which, in conventional methods, can lead to nonoptimal solutions.
4) The use of F_{ANN1} and F_{ANN2} in (3), being their inputs represented by the Belevitch canonical form, provides an automatic method to design both MNs considering the performance metrics for a specific bandwidth.
5) The proposed method (PM) can be extended for more complex amplification architectures, such as the Doherty PA.

III. Methodology Evaluation and Validation

To illustrate the proposed methodology, a class AB PA was designed using load- and source-pull simulated data from a 30-W GaN HEMT transistor, thus building (1) and (2). This will allow us to have a better perception of the differences and relative advantages of the PM without possible measurement errors.

Fig. 2 shows the fundamental and second-harmonic output terminations as black dots and red crosses, respectively, that were used to carry out load pull, being the inputs of F_{ANN1}. In Fig. 2(b), the gray crosses correspond to the input terminations used to assess the gain characteristic along with the fundamental output terminations, being the inputs of F_{ANN2}. Fig. 2 also shows a comparison of the efficiency, P_{out}, and gain contours obtained from the nonlinear circuit model and from the extracted ANN models at 2.4 GHz.

The performance of the PM was compared with the one obtained using a state-of-the-art broadband design technique, the SRFT, with a modification to ensure fairness: besides considering the fundamental impedances, it also tries to force the second-harmonic reflection coefficient to be in the edge

TABLE I

CHARACTERISTIC IMPEDANCES AND FREQUENCIES OBTAINED FOR THE IMN AND OMN OF THE DIFFERENT METHODS

	Z_{01} (Ω)	Z_{02} (Ω)	Z_{03} (Ω)	Z_{04} (Ω)	Z_{05} (Ω)	Z_{06} (Ω)	Z_{07} (Ω)	Z_L (Ω)	F_C (GHz)
PM (OMN)	52	22	3.3	8.8	65	15	32	47.7	10.9
$SRFT_{Eff}$ (OMN)	71	20	4.4	4.2	101	32	29	92.3	11.7
$SRFT_{Pout}$ (OMN)	72	25	3.8	5.7	110	27	35.5	93.2	12.2
PM (IMN)	11	55	19	33	31.5	69	52	71.3	7.9

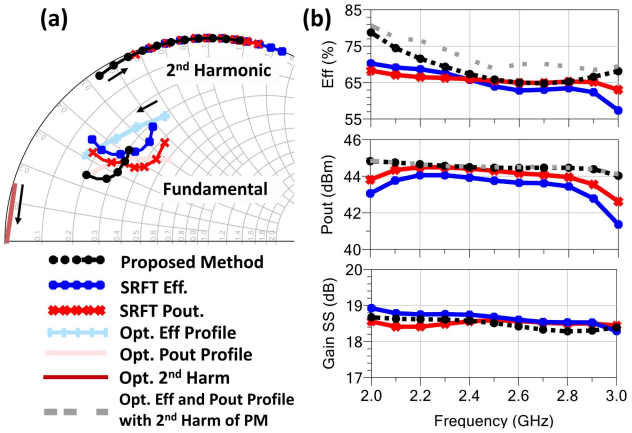

Fig. 3. (a) Fundamental and second-harmonic impedance profiles of the different methods along with the ones for optimum efficiency and output power. (b) Efficiency, output power (at 3 dB compression), and small-signal gain over frequency for all methods.

of the Smith chart. The SRFT was applied twice: first to achieve the optimum efficiency profile and second to get the optimum power profile. From now on, these two variants will be referenced as SRFT_{Eff} and $\text{SRFT}_{P_{\text{out}}}$, respectively. The MN's structure, considered for the applied methods, was composed by six cascaded transmission lines and by a parallel stub terminated in a short circuit.

In the PM, the following objectives were defined as follows: $\text{Gain}_{\text{SS}} \geq 17.5$ dB; $\text{Eff}_{3\,\text{dB}} \geq 65\%$; and $P_{\text{out3\,dB}} \geq 43.5$ dBm. After adjusting the objective function's weights, the characteristic impedances obtained for the OMN elements were compared with the other methods (Table I) and the corresponding PA metrics were analyzed (Fig. 3). The used initial conditions and optimization method were the same for all compared approaches. Beyond that, please note that, since the IMN for both SRFT tests needed to be separately optimized to evaluate the three PAs, we decided to use the IMN obtained from the PM in all of them, which is also presented in Table I. The efficiency and P_{out} were evaluated at the same compression level (3 dB).

The fact that Z_L obtained from the methods is not 50 Ω is related to the zero at dc defined in the $f(\lambda)$ polynomial [9]. This means that we will have to do a real-to-real matching later on.

From Fig. 3, we can observe that, besides the PM requiring much less time and human intervention, it also achieves a performance close to the optimum ones (dashed gray line). Moreover, as we expected, the performance of the PM is better than the SRFT approaches, which highlights the importance of a proper impedance selection, a task that is automatically performed by our PM, without the PA designer's intervention.

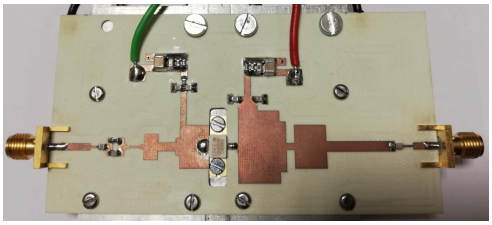

Fig. 4. Fabricated wideband PA.

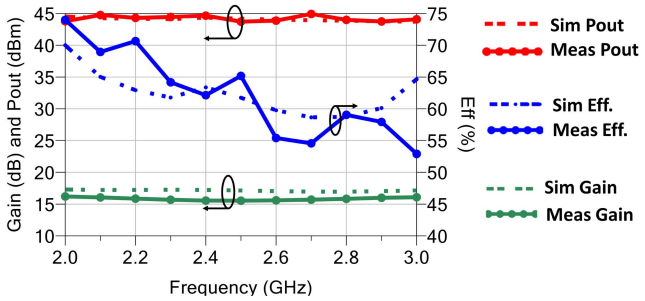

Fig. 5. Comparison between electromagnetic (EM) simulation and measurements of output power, efficiency, and small-signal gain over frequency.

The validation of the method was carried out by implementing the PA with the MNs presented in Table I. The characteristic impedances and the electrical lengths of the ideal lines were first converted to the corresponding widths and lengths, according to the used substrate. Then, these values had to be trimmed due to the discontinuities between consecutive transmission lines. As already mentioned, Z_L of the MNs is not 50 Ω, which is necessary for a real-to-real impedance transformation. Beyond that, we have also considered the dc block and the *RC* parallel circuit (in IMN, due to PA stability).

The final fabricated PA is shown in Fig. 4, and the comparison between simulated and measured efficiency, P_{out}, and gain (over frequency) is shown in Fig. 5.

Although the measured small-signal gain is lower than the simulated one, which may indicate some imprecision in the PA implementation, there is a good agreement between the simulated and measured P_{out} and efficiency over frequency.

As already mentioned, the PM can be extended for more complex configurations, such as the Doherty, where the MNs are designed for two power levels. For that, our methodology can be integrated into the one proposed in [11], in which the conventional SRFT is applied to this design problem. However, instead of optimizing the MNs to achieve the desired back off and full power loads, we can directly optimize the MNs to achieve the desired power levels with the best possible efficiency, avoiding the issues inherent to the preselection of the impedance profiles.

IV. CONCLUSION

This work proposes an automatic design methodology that uses a multidimensional search algorithm to find the best compromise between fundamental and harmonic impedances and, simultaneously, directly optimizes the PA MNs (that can be systematically synthesized) to obtain the desired gain, efficiency, and P_{out} metrics. The method avoids a blind pursuit of the optimum impedances and the need for having a nonlinear circuit model. Although validated for a single-ended PA, the method can be extended to more complex amplification architectures.

REFERENCES

[1] B. S. Yarman and H. J. Carlin, "A simplified 'real frequency' technique applied to broad-band multistage microwave amplifiers," *IEEE Trans. Microw. Theory Techn.*, vol. MTT-30, no. 12, pp. 2216–2222, Dec. 1982.

[2] X. Hu, X. Meng, C. Yu, and Y. Liu, "Design of highly efficient broadband harmonic-optimised GaN power amplifier via modified simplified real frequency technique," *Electron. Lett.*, vol. 53, no. 21, pp. 1414–1416, Oct. 2017.

[3] Y. Sun and X. Zhu, "Broadband continuous class F^{-1} amplifier with modified harmonic-controlled network for advanced long term evolution application," *IEEE Microw. Wireless Compon. Lett.*, vol. 25, no. 4, pp. 250–252, Apr. 2015.

[4] P. Chen, B. M. Merrick, and T. J. Brazil, "Bayesian optimization for broadband high-efficiency power amplifier designs," *IEEE Trans. Microw. Theory Techn.*, vol. 63, no. 12, pp. 4263–4272, Dec. 2015.

[5] P. Chen, J. Xia, B. M. Merrick, and T. J. Brazil, "Multiobjective Bayesian optimization for active load modulation in a broadband 20-W GaN Doherty power amplifier design," *IEEE Trans. Microw. Theory Techn.*, vol. 65, no. 3, pp. 860–871, Mar. 2017.

[6] K. Tran, R. Henderson, and J. Gengler, "Design of a 1–2.8-GHz 100-W power amplifier with bounded performance technique," *IEEE Trans. Microw. Theory Techn.*, vol. 67, no. 9, pp. 3707–3715, Sep. 2019.

[7] L. Kouhalvandi, M. Pirola, and S. Ozoguz, "Automated two-step power amplifier design with pre-constructed artificial neural network," in *Proc. 43rd Int. Conf. Telecommun. Signal Process. (TSP)*, Milan, Italy, Jul. 2020, pp. 617–620.

[8] L. Kouhalvandi, O. Ceylan, and S. Ozoguz, "Automated deep neural learning-based optimization for high performance high power amplifier designs," *IEEE Trans. Circuits Syst. I, Reg. Papers*, vol. 67, no. 12, pp. 4420–4433, Dec. 2020.

[9] S. Yarman, *Design of Ultra Wideband Power Transfer Networks*. New York, NY, USA: Wiley, 2010.

[10] Z. Dai, S. He, F. You, J. Peng, P. Chen, and L. Dong, "A new distributed parameter broadband matching method for power amplifier via real frequency technique," *IEEE Trans. Microw. Theory Techn.*, vol. 63, no. 2, pp. 449–458, Feb. 2015.

[11] F. Meng, X.-W. Zhu, J. Xia, and C. Yu, "A new approach to design a broadband Doherty power amplifier via dual-transformation real frequency technique," *IEEE Access*, vol. 6, pp. 48588–48599, 2018.